American Journal of Physical Chemistry
2014; 3(5): 61-66
Published online October 30, 2014 (http://www.sciencepublishinggroup.com/j/ajpc)
doi: 10.11648/j.ajpc.20140305.12
ISSN: 2327-2430 (Print); ISSN: 2327-2449 (Online)

Characterization of electrochemical cycling-induced new products of $NaCuO_2$ cathode material for sodium secondary batteries

Yoko Ono[1, 2, *], Yuhki Yui[1], Kaoru Asakura[1], Jiro Nakamura[1], Masahiko Hayashi[1, 2], Kazue Ichino Takahashi[1, 2]

[1]Energy and Environment Systems Laboratories, NTT Corporation, Kanagawa 243-0198, Japan
[2]Graduate School of Natural Science and Technology, Kanazawa University, Kanazawa, Ishikawa 920-1192, Japan

Email address:
ono.yoko@lab.ntt.co.jp (Y. Ono)

To cite this article:
Yoko Ono, Yuhki Yui, Kaoru Asakura, Jiro Nakamura, Masahiko Hayashi, Kazue Ichino Takahashi. Characterization of Electrochemical Cycling-Induced New Products of $NaCuO_2$ Cathode Material for Sodium Secondary Batteries. *American Journal of Physical Chemistry.* Vol. 3, No. 5, 2014, pp. 61-66. doi: 10.11648/j.ajpc.20140305.12

Abstract: Using a Na/$NaCuO_2$ cell, we investigate the conversion of $NaCuO_2$ during charge and discharge reactions and the new products formed by the conversion. In the voltage range of 0.75 to 3.0 V, the results of ex-situ XRD analysis indicate that Na_2CuO_2, an unstable amorphous discharge product, converted into CuO and Cu_2O. Moreover, an XPS analysis reveals Na_2O is formed on the surface of a $NaCuO_2$ electrode. From 1.7 to 4.2 V, on the other hand, the first charge product, $Na_{1-x}CuO_2$, should partially form CuO. This behavior is similar to the reaction in which the charge of a Li/$LiCuO_2$ cell forms CuO. Then, after the discharge, CuO and Cu_2O are observed as the main components in XRD patterns of the electrode. $NaCuO_2$ phase appeared again after the subsequent charge. $NaCuO_2$ is gradually converted into CuO as the main component as the cycles proceed. The cycling-induced new products of $NaCuO_2$ change, depends on the voltage ranges.

Keywords: XRD Analysis, Sodium Copper Oxide, Metal Oxide Cathode, Sodium-Ion Batteries

1. Introduction

Lithium-ion secondary batteries (LIBs) are widely used owing to their high voltages and high energy density. However, alternatives to LIBs are being sought because of the scarcity of lithium resources. Sodium-ion secondary batteries (SIBs) have attracted much attention as an alternative to LIBs because of the abundance of sodium resources. Recently, various cathode materials for SIBs have been investigated, and, among them, transition metal compounds with layered structure are promising. While Na_xCoO_2 [1], $NaCrO_2$ [2,3], Na_xMnO_2 [4-6] and $NaNi_{1/2}Mn_{1/2}O_2$ [7] have been reported as high performance cathodes, there are few reports about copper oxide as a cathode material.

We have recently focused on $NaCuO_2$ as a cathode material for SIBs and have reported the charge-discharge properties using a Na/$NaCuO_2$ cell [8]. While $NaCuO_2$ has small discharge capacity and low rechargeability as an LIB cathode material [9], we found that $NaCuO_2$ has a potential to be used as an SIB cathode material. Theoretically, sodium-ion insertion and extraction from $NaCuO_2$ respectively correspond to the reduction of Cu^{3+} to Cu^{2+} and the oxidation of Cu^{3+} to Cu^{4+} as

$$NaCu^{3+}O_2 + xNa^+ + xe^- \rightarrow Na_{1+x}Cu^{2+}O_2 \quad (1)$$

$$NaCu^{3+}O_2 \rightarrow Na_{1-x}Cu^{4+}O_2 + xNa^+ + xe^- \quad (2)$$

In our experiments, when the Na/$NaCuO_2$ cell was discharged from open circuit voltage (OCV) of 2.7 to 0.75 V, sodium-ion insertion into $NaCuO_2$ proceeded with the first discharge capacity of 140 mAh/g (x = 0.6 in $Na_{1+x}CuO_2$, The value x was calculated from theoretical capacity of 226 mAh/g.). As for the cycle properties, noticeable fading of discharge capacity during the cycles was observed. On the other hand, when the cell was charged from OCV of 2.7 to 4.2 V, sodium-ion extraction from $NaCuO_2$ occurred with the first charge capacity of 134 mAh/g (x = 0.6 in $Na_{1-x}CuO_2$). Except for the first charge, the charge and discharge capacities

gradually increased. These capacity changes with cycles suggested side reactions that involve the decomposition of $NaCuO_2$ and the formation of new charge/discharge products during the charge and discharge processes. For $LiCuO_2$ as an LIB cathode material, which has the same crystal structure as $NaCuO_2$, it has been known that $LiCuO_2$ is converted to CuO_2, CuO and Li_xCuO as charge/discharge products.

In this study, we reveal the reaction mechanism of $NaCuO_2$ and discuss the difference between $NaCuO_2$ and $LiCuO_2$. An X-ray diffraction (XRD) analysis of $NaCuO_2$ electrodes was performed at various charged/discharged stages to clarify the new charge/discharge products of $NaCuO_2$. The conversion of $NaCuO_2$ was investigated in the voltage ranges of 0.75 to 3.0 V (started with discharge) and 1.7 to 4.2 V (started with charge).

2. Experimental

2.1. Synthesis and Characterization of $NaCuO_2$ Powder

$NaCuO_2$ was synthesized by solid-state calcination. Reagent grade Na_2O_2 (Kanto Chemical Co.) and CuO (Kanto Chemical Co.) were mixed with a molar Na/Cu ratio of 1.0 and then calcinated at 450°C for 10 h in an oxygen gas flow as reported elsewhere [9]. After calcination, the sample was removed from the furnace with the temperature at 100°C and stored in a dry air atmosphere (dew point < −50°C). The obtained sample was characterized by XRD (Rigaku, X-ray diffractometer RINT2000) using CuKα radiation, and the morphology of the sample was observed with a scanning electron microscope (SEM) (Hitachi High-Technologies Co., SU1510) with accelerating voltage of 15.0 kV.

2.2. Cell Fabrication and Electrochemical Measurements

The electrochemical properties of $NaCuO_2$ were evaluated using 2032 coin cells (Hosen Co.). As a working electrode, a mixture of 75 wt% $NaCuO_2$, 13.5 wt% acetylene black (Denka Co.), 1.5 wt% Ketjen Black EC600JD (Lion Co.), and 10 wt% polyvinylidene difluoride (PVDF) (Daikin Industries ltd) in N-methylpyrrolidone was pasted on alminum foil as a current collector and dried at 90°C overnight. Then it was pressed at 100 °C and punched out. The counter electrode was a sodium metal disc, which was cut from sodium cubes (Kanto Chemical Co.), pressed, punched out, and washed with propylene carbonate. The electrolyte solution was 1 mol/l $NaClO_4$ dissolved in propylene carbonate (PC, Tomiyama Pure Chemicals Industries, Ltd.). The cells were assembled in a glove box filled with argon gas (dew point < −75°C). Electrochemical measurements were carried out at a constant current density of 0.03 mA/cm^2 (5.0 mA/g) at 25°C.

2.3. Characterization of $NaCuO_2$-Containing Electrode after Charge/Discharge

After the charge/discharge process, $NaCuO_2$-containing electrodes were removed from charged/discharged coin cells and washed with dimethyl carbonate in the glove box. Then they were dried in the glove box overnight.

The crystal structure of $NaCuO_2$-containing electrodes before and after charge/discharge processes was determined by XRD analysis. Scanning electron microscopy-energy dispersion X-ray spectrometry (SEM-EDS) was used to observe the surface/cross-section structure and analyze the composition of the $NaCuO_2$ electrodes. The measurements were performed with an ULTRA55(SEM) (Carl Zeiss Co.) and QUANTAX400 (BRUKER Co.), with accelerating voltage of 3.0 kV. EDS maps of elemental compositions were obtained from SEM images. An X-ray photoelectron spectrometer (XPS) analysis of the samples was performed with a PHI XPS-5700 system using AlKα radiation (1486.6 eV) to examine the binding energy for Na 1s, Cu 2p and O 1s of $NaCuO_2$ electrodes. Sputtering was performed using Ar^+ with accelerating voltage of 3.0 kV to analyze the depth profiles of the electrodes. The sputtering rate was 2.7 nm/min.

3. Results and Discussion

3.1. Characterization of $NaCuO_2$ Powder

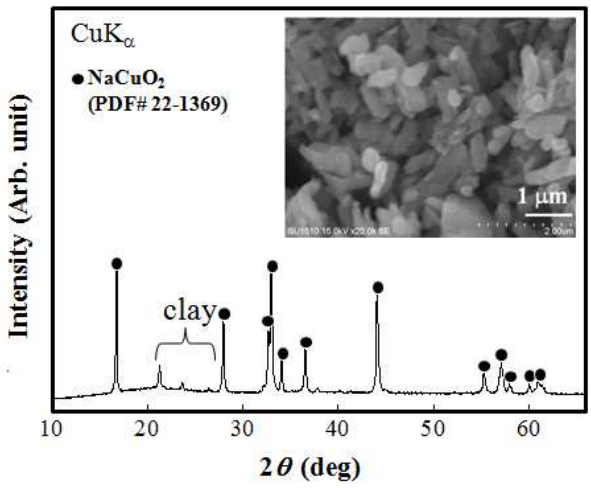

Figure 1. *XRD pattern of obtained powder. Clay was used to set the powder to the XRD sample holder. Inset: SEM image of $NaCuO_2$ powder.*

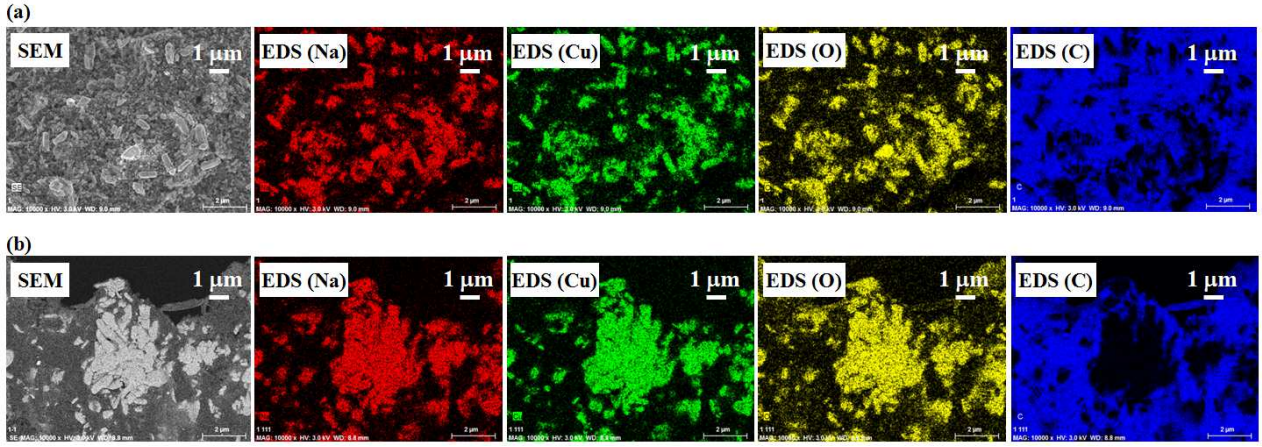

Figure 2. *SEM images and EDS elemental mapping images of (a) surface and (b) cross section of $NaCuO_2$ electrode. The section of the sample was prepared by cutting the electrode with a cutter knife.*

Figure 1 shows the powder XRD pattern of the sample obtained at 450°C for 10 h in oxygen. The XRD pattern of the sample was indexed to a $NaCuO_2$ phase (PDF # 22-1369), and it is consistent with the pattern reported in the literature [9]. This result indicates $NaCuO_2$ was obtained as a single phase. The structure of $NaCuO_2$ has been reported as monoclinic [10]. In an SEM image of the obtained $NaCuO_2$ powder (inset in Fig. 1), rice-grain-like particles with the size of 0.5 – 1.0 μm were observed. The XRD pattern of the as-prepared $NaCuO_2$-containing electrode was not different from that of the $NaCuO_2$ powder.

Figure 2 shows SEM images and EDS elemental mapping images of the as-prepared $NaCuO_2$ electrodes. The EDS maps were obtained for Na, Cu, O and C elements. SEM-EDS measurements of the electrode surface indicate that about 1 μm size of $NaCuO_2$ particle was dispersed [Fig. 2 (a)]. There was no segregation of Na, Cu, O, and C, and no impurities, such as Na_2CO_3 and CuO, were observed. In the cross-sectional image [Fig. 2 (b)], aggregates of $NaCuO_2$ with a size of approximately 5 μm were observed.

3.2. New Charge/Discharge Products of $NaCuO_2$-Containing Electrode during Charge-Discharge in the Range of 0.75 – 3.0 V (Started with Discharge)

Figure 3 (a) shows the first and second discharge-charge curves of a Na/$NaCuO_2$ cell in the voltage range of 0.75 to 3.0 V. The first discharge capacity was 140 mAh/g (corresponding to 0.6 mol of sodium-ion insertion; $Na_{1.6}CuO_2$), and the average discharge voltage was 1.7 V. As we have previously reported [8], the second discharge capacity drastically decreased to 90 mAh/g. To investigate the reason for the decrease in capacity, we performed a structural analysis of $NaCuO_2$ at the discharged/charged stage.

Figure 3 (b) shows XRD patterns of $NaCuO_2$ electrodes after the first discharge [Fig. 3 (a)-(i)] and the subsequent charge processes [Fig. 3 (a)-(ii)]. After the first discharge, the $NaCuO_2$ peaks almost completely disappeared, and new peaks assigned to CuO and Cu_2O were observed [Fig. 3 (b)-(i)]. However, the $Na_{1.6}CuO_2$ phase, which is considered to be the discharge product, could not be observed. This XRD pattern was retained after the subsequent charge process [Fig. 3 (b)-(ii)]. From the results of the XRD analysis during the first cycle, we suggest following reaction mechanism.

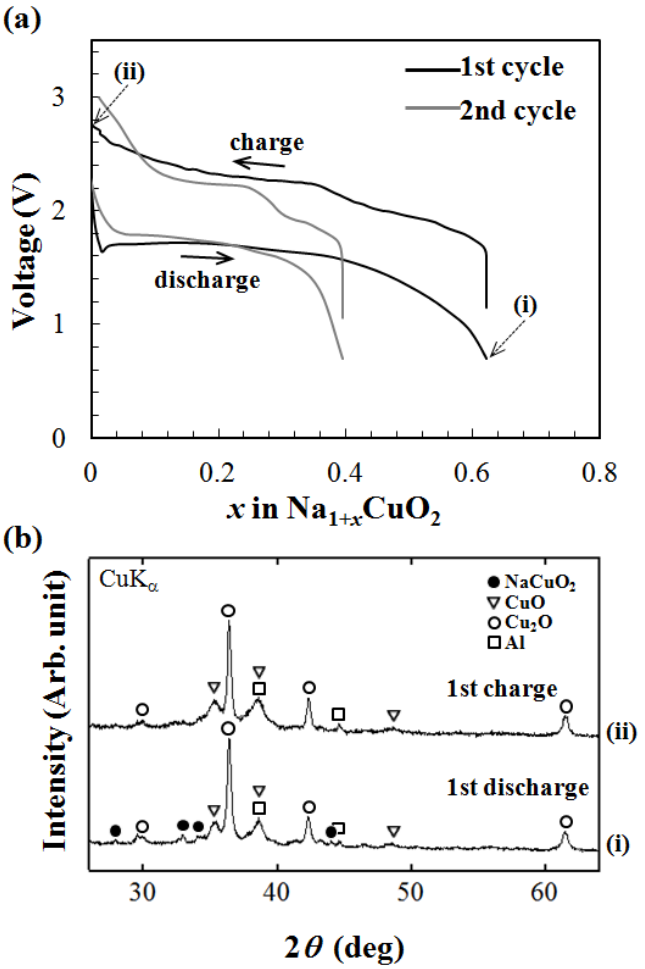

Figure 3. *(a) First and second discharge–charge curves of a Na/$NaCuO_2$ cell at 0.75–3.0 V. (b) XRD patterns of the $NaCuO_2$ electrodes after the (i) first discharge and (ii) first charge processes [see Fig. 3 (a)].*

Sodium-ion insertion into $NaCuO_2$ during the first discharge involves irreversible conversion of $NaCuO_2$ to the amorphous phase, Na_2CuO_2. Then, charge and discharge reactions between the amorphous phases proceed. On the other hand, the discharge product, Na_2CuO_2 ($Na_{1.6}CuO_2$, to be exact), which was formed through the reaction

$$NaCuO_2 + Na^+ + e^- \rightarrow Na_2CuO_2 \quad (3)$$

might be unstable and decompose to form copper oxide and sodium oxide:

$$Na_2CuO_2 \rightarrow Na_2O + CuO \quad (4)$$

Then, CuO reacts with sodium-ion and produces Cu_2O and Na_2O:

$$CuO + Na^+ + e^- \rightarrow 1/2\ Cu_2O + 1/2\ Na_2O \quad (5)$$

The instability of Na_2CuO_2 might be one reason for the poor cycle performance. However, Na_2O could not to be detected by an XRD analysis of the $NaCuO_2$ electrode after the first discharge. Since Na_2O was in the amorphous phase, XPS measurement was carried out for discharged $NaCuO_2$ electrodes to analyze the chemical states of the Na in the oxide.

Figure 4 shows Na1s XPS spectra of the $NaCuO_2$ electrodes before and after the first discharge to 0.75 V. While the binding energy of the Na1s main peak was observed with the maximum intensity at 1072.0 eV before the discharge [Fig. 4 (i)], the peak shifted to 1072.3 eV after the discharge [Fig. 4 (ii)]. This peak at 1072.3 eV is considered to be the sum of Na1s peaks for both the discharge products and unreacted $NaCuO_2$. The components of the peak were therefore identified by multi-peak fitting. The observed peak was separated into two peaks, as shown by the dotted line in Fig. 4 (ii). One peak had its maximum binding energy at 1072.7 eV, which was assigned to Na_2O according to a reference [11], and the other had its maximum at 1072.0 eV and was assigned to $NaCuO_2$. The intensity ratio of peaks at 1072.7 and 1072.0 eV was 6:4. The ratio is in agreement with the amount of reacted $NaCuO_2$ and 0.6 mol and unreacted $NaCuO_2$ of 0.4 mol, calculated from the first discharge capacity of 140 mAh/g. No clear peak for Cu2p was detected before or after the first discharge because of its low intensity at the surface of the $NaCuO_2$ electrode. Figure 5 shows the depth profiles of the intensity of the binding energy for Na1s, Cu2p, and O1s of $NaCuO_2$ electrodes after the first discharge to 0.75 V. At the surface of the $NaCuO_2$ electrode, Na1s and O1s were the dominant components and the binding energy of Cu2p could not be detected. This result indicates that the discharged product, Na_2O, might cover the surface of the $NaCuO_2$ electrode. At deeper positions, the intensity of Na1s decreased and that of Cu2p increased.

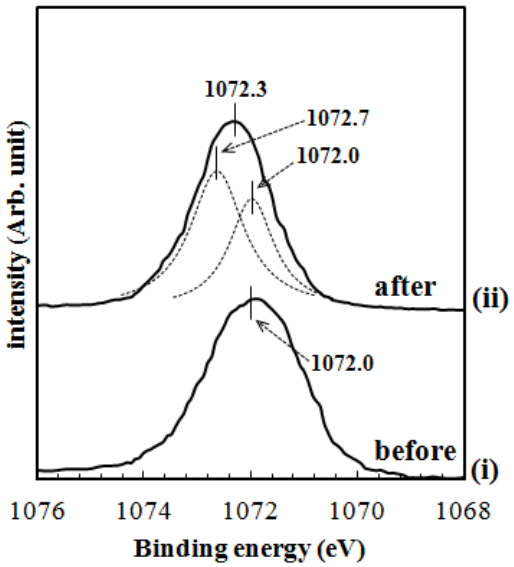

Figure 4. *XPS spectra of Na1s for the $NaCuO_2$ electrodes (i) before and (ii) after the first discharge to 0.75 V. The test of a Na/$NaCuO_2$ cell started with the discharge process. Dotted lines show fitting Lorenz curves obtained by multi peak fitting with IGOR Pro.*

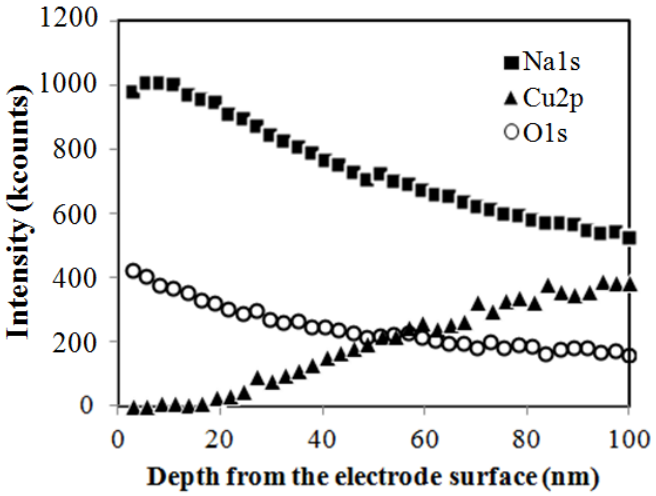

Figure 5. *Depth profiles of the intensity of binding energy for Na1s, Cu2p, and O1s of $NaCuO_2$ electrodes after the first discharge to 0.75 V. The depth was calculated from the sputtering rate of 2.7 nm/min.*

In summary, it was revealed that sodium-ion insertion into $NaCuO_2$ formed unstable Na_2CuO_2, which was converted to Cu_2O after decomposition into CuO. Moreover, Na_2O was also formed on the surface of the $NaCuO_2$ electrode.

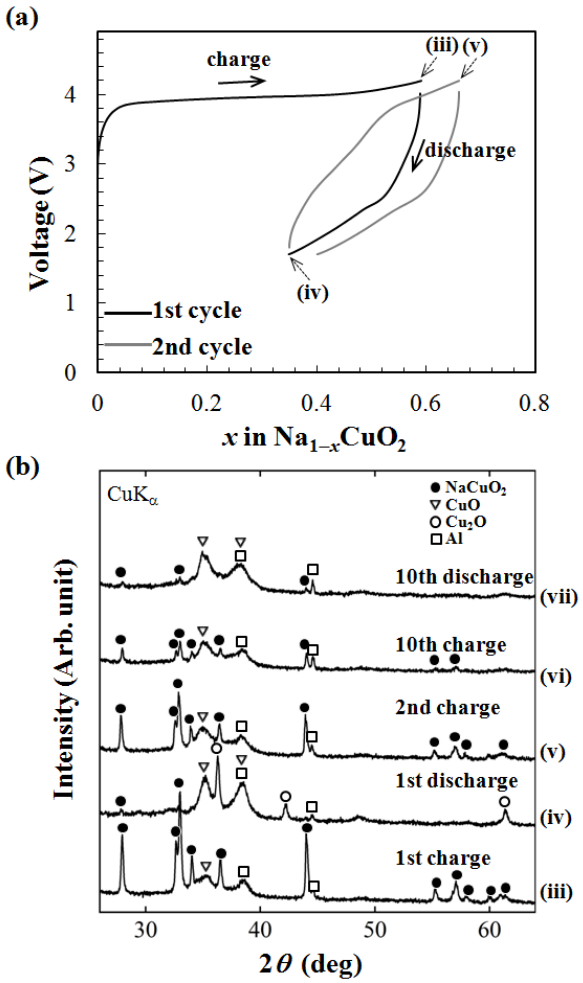

Figure 6. *(a) First and second charge–discharge curves of a Na/$NaCuO_2$ cell at 1.7–4.2 V. (b) XRD patterns of the $NaCuO_2$ electrodes after the (iii) first charge, (iv) first discharge and (v) second charge together with the pattern after (vi), (vii) the tenth charge-discharge process.*

3.3. New Charge/Discharge Products of $NaCuO_2$-Containing Electrode during Charge-Discharge in the Range of 1.7 – 4.2 V (Started with Charge)

Figure 6 (a) shows the first and second charge-discharge curves of a Na/$NaCuO_2$ cell in the voltage range of 1.7 to 4.2 V. The first charge and discharge capacities were 134 mAh/g (corresponding to 0.6 mol of sodium-ion extraction; $Na_{0.4}CuO_2$) and 55 mAh/g (corresponding to 0.2 mol of sodium-ion insertion; $Na_{0.6}CuO_2$), respectively, and the average discharge voltage was 2.5 V. The curve shapes changed after the first cycle. This behavior is very similar to the results for lithium-ion extraction in a Li/$LiCuO_2$, Li/$Li_{1.5}CuO_2$ and Li/Li_2CuO_2 cells [12-14].

Figure 6 (b) show XRD patterns of $NaCuO_2$ electrodes after the first charge (iii) and discharge (iv) and the subsequent charge (v). The XRD patterns after the tenth charge-discharge process are also shown [(vi) and (vii)]. After the first charge, $NaCuO_2$ retained its pattern and a broad peak assigned to CuO appeared [Fig. 6 (b)-(iii)]. The formation of CuO is similar to the behavior that the first charge process of $LiCuO_2$ forms CuO_2, and that CuO_2 converts to CuO [13]. Therefore, $NaCuO_2$ should form the CuO_2 phase by sodium-ion extraction from $NaCuO_2$ by the reaction in Eq. (2), but CuO_2 could not be detected because of its conversion to CuO. After the subsequent discharge, the $NaCuO_2$ peaks almost completely disappeared and the peak intensities attributed to CuO increased and new peaks assigned to Cu_2O appeared [Fig. 6 (b)-(iv)]. For the $LiCuO_2$ system, Arachi et al. reported that CuO, which was formed by 1 mol of lithium-ion extraction from $LiCuO_2$, reacts with lithium ions and then forms LiCuO and Cu [12]. Their results support a possible reaction between CuO and sodium ions. However, in the $NaCuO_2$ system, the Na_xCuO phase could not be detected after the discharge process because of the low discharge capacity (x = 0.2) or low crystallinity of Na_xCuO. Then, after the second charge, the $NaCuO_2$ phase appeared again [Fig. 6 (b)-(v)]. The $NaCuO_2$ peaks gradually faded during the cycles, and broad CuO peaks were observed as the main peaks after ten cycles, as shown in Fig. 6 (vi) and (vii). The results indicate that the CuO phase, which was observed at 1.75 V, is more stable than $NaCuO_2$ formed at higher voltage (4.2 V). Therefore, $NaCuO_2$ was transformed into CuO during cycles.

In summary, we found that, during the charge and discharge reactions, the decomposition and charge/discharge products of $NaCuO_2$ differ from those in the $LiCuO_2$ system. While the $LiCuO_2$ system is irreversibly converted to CuO during the first charge, $NaCuO_2$ reversibly changes between $NaCuO_2$ and CuO during the first charge-discharge and the subsequent second charge precesses.

3.4. Comparison of Charge/Discharge Reaction Products for Li_xCuO_2 and $NaCuO_2$ Electrode Systems

Figure 7 shows the reaction pathway and new products during the first charge/discharge process for Li_xCuO_2 (x = 1, 2) and $NaCuO_2$ electrode systems in Li/Li_xCuO_2 and Na/$NaCuO_2$ cells, respectively. Normal electrode potential vs. SHE are shown as the main axis, and the voltages vs. Li/Li^+ and Na/Na^+ are also shown. For the $NaCuO_2$ electrode, CuO (about 4.0, 1.7 and 0.75 V vs. Na/Na^+), Cu_2O (about 1.7 and 0.75 V vs. Na/Na^+) and Na_2O (about 0.75V vs. Na/Na^+) are observed after the first charge-discharge processes, while the NaCuO phase could not be observed. CuO produced after the first charge to 4.2 V is reversibly converted to $NaCuO_2$ phase after the second cycle. For the Li_xCuO_2 electrode, on the other hand, charge/discharge processes form LiCuO (about 2.5V vs. Li/Li^+), Cu (about 1.8 V vs. Li/Li^+) and Li_2O (about 1.8 V) in addition to CuO (about 2.5 V vs. Li/Li^+). CuO formed after the first charge to 4.3 V could not be converted to $LiCuO_2$. While charge/discharge products of Cu^{3+}, Cu^{2+} and Cu^{1+} compounds are observed as the charge/discharge products including the initial states in both Li_xCuO_2 and $NaCuO_2$ systems. However, NaCuO could not be observed in the $NaCuO_2$ system because of different stability of LiCuO and NaCuO. Since the stability of sodium lithium ions in the lattice of $NaCuO_2$ and $LixCuO_2$ should be affected by the different electrode potential vs. SHE and the ionic radius of

each ion, $NaCuO_2$ and $LixCuO_2$ exhibit different reaction pathway. For future study, it is worth investigating in the wide voltage range, taking into consideration the higher overvoltage characteristics of SIBs, and examining the possibility of NaCuO formation at around 2.5 V (vs. Na/Na^+) to gain a detailed understanding of the reaction mechanism.

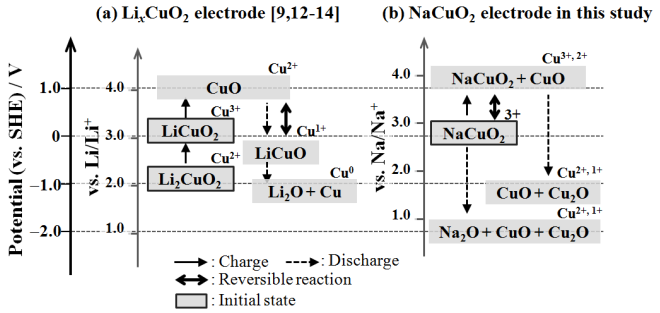

Figure 7. *Schematic illustration of the reaction pathway and new products during the first charge/discharge process for (a) Li_xCuO_2 [9,12-14] and (b) $NaCuO_2$ electrode systems.*

4. Conclusion

We synthesized $NaCuO_2$ as a cathode material for an SIB, and examined the formation of new products during charge and discharge reactions in voltage ranges of 0.75 to 3.0 V and 1.7 to 4.2 V. Sodium-ion insertion into $NaCuO_2$ (the first discharge to 0.75 V of a $Na/NaCuO_2$ cell) involved the formation of CuO and Cu_2O. Na_2O was also formed on the surface of the $NaCuO_2$ electrode. On the other hand, sodium-ion extraction from $NaCuO_2$ (the first charge to 4.2 V of a $Na/NaCuO_2$ cell) suggested the conversion of the charged product, CuO_2, to CuO. This conversion behavior is similar to the reaction in which the charge of a $Li/LiCuO_2$ cell forms CuO. After the subsequent discharge-charge process, the XRD pattern of the $NaCuO_2$ phase was observed again, and then the $NaCuO_2$ peaks gradually faded with the cycles. We found that reaction products of $NaCuO_2$ differ from those of the Li_xCuO_2 system and that $NaCuO_2$ is converted to CuO, Cu_2O, and Na_2O during charge and discharge depending on the voltage ranges.

References

[1] R. Berthelot, D. Carlier and C. Delmas, "Electrochemical investigation of the P2–Na_xCoO_2 phase diagram," *Nat. Mater.*, 2011, 74, pp. 74–80.

[2] S. Komaba, C. Takei, T. Nakayama, A. Ogata and N. Yabuuchi, "Electrochemical intercalation activity of layered $NaCrO_2$ vs. $LiCrO_2$," *Electrochem. Commun.* 2010, 12, pp. 355–358.

[3] X. Xia and J.R. Dahn, "$NaCrO_2$ is a fundamentally safe positive electrode material for sodium-ion batteries with liquid electrolytes," *Electrochem. Solid State Lett.*, 2012, 15(1), A1–A4.

[4] X. Ma, H.Chen and G. Ceder, "Electrochemical properties of monoclinic $NaMnO_2$," *J. Electrochem. Soc.*, 2011, 158, A1307–A1312.

[5] R. Stoyanova, D. Carlier, M. Sendova-Vassileva, M. Yoncheva, E. Zhecheva, D. Nihtianova and C. Delmas, "Stabilization of over-stoichiometric Mn^{4+} in layered $Na_{2/3}MnO_2$," *J. Solid State Chem.*, 2010, 183, pp. 1372–1379.

[6] H. Kim, D.J. Kim, D.H. Seo, M.S. Yeom, K. Kang, D.K. Kim and Y. Jung, "Ab initio study of the sodium intercalation and intermediate phases in $Na_{0.44}MnO_2$ for sodium-ion battery," *Chem. Mater.*, 2012, 24, pp. 1205–1211.

[7] S. Komaba, T. Nakayama, A. Ogata, T. Shimizu, C. Takei, S. Takada, A. Hokura and I. Nakai, "Electrochemically reversible sodium intercalation of layered $NaNi_{0.5}Mn_{0.5}O_2$ and $NaCrO_2$," *ECS Trans.*, 2008, 16 (42), pp. 43–55.

[8] Y. Ono, Y. Yui, M. Hayashi, K. Asakura, H. Kitabayashi, K. I. Takahashi, "Electrochemical properties of $NaCuO_2$ for sodium-ion secondary batteries," *ECS Trans.*, 2014, 58 (12), pp. 33–39.

[9] H. Arai, S. Okada, Y. Sakurai and J. Yamaki, "Electrochemical and structural study of Li_2CuO_2, $LiCuO_2$ and $NaCuO_2$," *Solid State Ion.*, 1998, 106, pp. 45–53.

[10] N.E. Brase, M. O'Keeffe, R.B. von Dreele,V.G. Young Jr., "Crystal structures of $NaCuO_2$ and $KCuO_2$ by neutron diffraction," *J. Solid State Chem.*, 1989, 83, pp. 1–7.

[11] A. Barrie and F.J. Street, "An Auger and X-ray photoelectron spectroscopic study of sodium metal and sodium oxide," *J. Electron Spectrosc. Relat. Phenom.*, 1977, 7, pp. 1–30.

[12] Y. Arachi, T. Setsu, T. Ide, K. Hinoshita and Y. Nakata, "Reversible electrochemical reaction of CuO with Li in the $LiCuO_2$ system," *Solid State Ionics*, 2012, 225, 611–614.

[13] E. A. Reakelboom, A.L. Hector, M.T. Weller and J.R. Owen, "Electrochemical properties and structures of the mixed-valence lithium cuprates $Li_3Cu_2O_4$ and $Li_2NaCu_2O_4$," *Journal of Power Source*, 2011, 97–98, pp. 465–468.

[14] Y. Arachi, Y. Nakata, K. Hinoshita, and T. Setsu, "Changes in electronic structure of $Li_{2-x}CuO_2$," Journal of Power Sources, 2011, 196, pp. 6939–6942.